

Depth-based reconstruction method for incomplete functional data

Antonio Elías Fernández* 

Department of Applied Mathematics
OASYS group
Universidad de Málaga

Raúl Jiménez

Department of Statistics
Universidad Carlos III de Madrid

Han Lin Shang 

Department of Actuarial Studies and Business Analytics
Macquarie University

Abstract

The problem of estimating missing fragments of curves from a functional sample has been widely considered in the literature. However, a majority of the reconstruction methods rely on estimating the covariance matrix or the components of its eigendecomposition, a task that may be difficult. In particular, the accuracy of the estimation might be affected by the complexity of the covariance function and the poor availability of complete functional data. We introduce a non-parametric alternative based on a novel concept of depth for partially observed functional data. Our simulations point out that the available methods are unbeatable when the covariance function is stationary, and there is a large proportion of complete data. However, our approach was superior when considering non-stationary covariance functions or when the proportion of complete functions is scarce. Moreover, even in the most severe case of having all the functions incomplete, our method performs well meanwhile the competitors are unable. The methodology is illustrated with two real data sets: the Spanish daily temperatures observed in different weather stations and the age-specific mortality by prefectures in Japan.

Keywords: Functional Data, Partially Observed Data, Reconstruction, Depth Measures.

1 Introduction

Partially observed functional data (POFD) are becoming more recurrent, invalidating many of the existing methodologies (Ramsay and Silverman, 2005; Ferraty and Vieu, 2006). Diverse case studies motivate the development of statistical tools for these types of data. For example, in medical studies, many data sets are recorded through periodical check-ups, and patients who miss

*Corresponding author: aelias@uma.es

appointments or devices that fail to record may be typical sources of censoring. These situations may present in different types of monitoring, such as ambulatory blood pressure, the health status of human immunodeficiency virus tests (HIV), growth curves, and the evolution of lung function (James et al., 2000; James and Hastie, 2001; Delaigle and Hall, 2013; Kraus, 2015; Delaigle and Hall, 2016). Sangalli et al. (2009, 2014) also consider POFD from aneurysm studies where the source of censoring comes from a prior reconstruction of the sample and posterior processing to make the data comparable across subjects. In demography, it is common that age-specific mortality rates for older ages are not completely observed due to the decreasing number of survivors (Human Mortality Database, 2021) and this cohort is the focus of actuarial science studies (D'Amato et al., 2011). Other examples involve electricity supply functions that may not be completely observed because suppliers and buyers typically agree on prices and quantities depending on the market conditions (Kneip and Liebl, 2020; Liebl and Rameseder, 2019).

Prominent literature has tackled estimating missing parts of partially observed functional data, providing several benchmark methods. Among them, the methods of Yao et al. (2005); Goldberg et al. (2014); Kraus (2015); Delaigle and Hall (2016); Kneip and Liebl (2020). In this article, a new method is presented and compared with two of the above benchmark methods. We selected those that provided the best performance to minimize the mean squared error on our simulations and considered case studies. The selected benchmark methods are the method of Kraus (2015), and the method of Kneip and Liebl (2020). Notably, Kraus (2015) proposes a functional linear ridge regression model for completing functional data based on principal component analysis. Kraus (2015) estimates the principal component scores of the incomplete functions from the completely observed functions and then uses a completion procedure for recovering the missing part of the functions by using the observed part. On the other hand, Kneip and Liebl (2020) approach the problem by introducing an optimal linear regression operator based on a local linear kernel aiming to produce smoother results and trying to avoid artificial jumps between observed and reconstructed parts.

Our approach combines two novel functional tools: 1) a depth-based method for functional time series forecasting (Elías et al., 2021c); and 2) a functional depth for partially observed functional data (Elías et al., 2021b).

The new method is conceived for: 1) Scenarios where the estimation of the covariance function is complex or impossible. We remark that the available reconstruction methods strongly depend on a proper estimation of the covariance. Its estimators might be very sensitive and become unreliable for many analyses, in particular for principal component analysis (Hubert et al., 2005). In addition, a low number of complete functions in the sample also hampers the estimation procedures and makes it impossible if all the sample functions are partially observed (Kneip and Liebl, 2020). 2) Reconstructing non-smooth functions. Some methods are designed to deal with smooth and

unaligned functions, and, in consequence, their results are smooth and aligned functions (Kneip and Liebl, 2020). Our goal is to provide a method that produces reconstructed functions remaining as accurate as possible in roughness and variability. 3) Adding interpretability. It might be useful to get a precise estimation and some insights into the final reconstruction drivers. We consider simulated and real data for illustrating the issues listed above. On the one hand, we consider yearly curves of Spanish daily temperatures. This data set is gathered at different weather stations spread along with the Spanish territory. On the other hand, we consider age-specific yearly mortality rates recorded at each Japanese prefecture (political territory division).

The structure of this paper is as follows: Section 2 introduces notation and the method. Section 3 shows a variety of simulated results based on Gaussian Processes under different simulated regimes of partial observability. In addition, we illustrate the method's performance with a Spanish daily temperatures data set and the Japanese age-specific mortality rates by prefecture. In Section 4, we make some conclusions.

2 Depth-based reconstruction method

2.1 Definition and notation

Let $X = \{X(t) : t \in [a, b]\}$ be a stochastic process of continuous trajectories and (X_1, \dots, X_n) independent copies of X . To simplify the notation, we assume without loss of generality $[a, b] = [0, 1]$. We consider the case X_1, \dots, X_n are partially observed. Following Delaigle and Hall (2013), we model the partially observed setting by considering a random mechanism Q that generates compact subsets of $[0, 1]$ where the functional data are observed. Specifically, let O be a random compact set generated by Q , and let (O_1, \dots, O_n) be independent copies of O . Therefore, for $1 \leq i \leq n$, the functional datum X_i is only observed on O_i . Let $(X_i, O_i) = \{X_i(u) : u \in O_i\}$, $M_i = [0, 1] \setminus O_i$ and (X_i, M_i) . Then, the observed and missing parts of X_i are (X_i, O_i) and (X_i, M_i) . We assume that $(X_1, O_1), \dots, (X_n, O_n)$ are i.i.d. realizations from $P \times Q$. This is, $\{X_1, \dots, X_n\}$ and $\{O_1, \dots, O_n\}$ are independent samples. This assumption, termed Missing-Completely-at-Random, is standard in the literature of POFD. Notedly, Liebl and Rameseder (2019) has considered a specific violation of the Missing-Completely-at-Random assumption.

The core idea of our method is based on the depth-based method for dynamic updating on functional time series (Elías et al., 2021c). In this context, but using the notation introduced here, the functional sample, (X_1, \dots, X_n) , was ordered in time, n being the most recent time period. X_n was only observed on $O_n = [0, q]$, with $0 \ll q < 1$, and the rest of sample curves $\{X_j : j < n\}$ were fully observed on $[0, 1]$. This is, for all $j < n$, $O_j = [0, 1]$. We may summarize the depth-based approach for dynamic updating as follows: if (X_n, O_n) is depth in $\{(X_j, O_n) : j \in \mathcal{J}_n\}$, for some

$\mathcal{J}_n \subset \{1, \dots, n-1\}$, and the band delimited by the curve segments $\{(X_j, O_n) : j \in \mathcal{J}_n\}$ captures both the shape and magnitude of (X_n, O_n) , we may estimate (X_n, M_n) from $\{(X_j, M_n) : j \in \mathcal{J}_n\}$. In particular, point estimators of (X_n, M_n) were obtained by computing weighted averages on the curve segments of $\{(X_j, M_n) : j \in \mathcal{J}_n\}$. In our jargon, $\{(X_j, O_n) : j \in \mathcal{J}_n\}$ is called the envelope of (X_n, O_n) .

In contrast to the dynamic updating framework described above, the sample curves may not be temporarily ordered in the partially observed scenario that we are considering. What is more important, every single curve may be partially observed. So, for enveloping the observed part of a curve, say us (X_i, O_i) , we could only have curve segments, namely $\{(X_j, O_i \cap O_j) : j \neq i\}$. Similarly, we may only have curve segments, specifically $\{(X_j, M_i \cap O_j) : j \neq i\}$, for estimating the missing part of X_i , that is (X_i, M_i) . How to apply the depth-based approach for these cases is a challenging problem that we address here. The method can be explained in two steps: one concerned about how to compute an *envelope* of (X_i, O_i) , described in Section 2.2 and one on how to estimate or reconstruct (X_i, M_i) from the observed parts of the curves used for enveloping (X_i, O_i) , described in Section 2.3.

2.2 A depth-based algorithm for focal-curve enveloping

This concept of depth arises for ordering multivariate data from *the center to outward* (Liu, 1990; Liu et al., 1999; Rousseeuw et al., 1999; Zuo and Serfling, 2000; Serfling, 2006; Li et al., 2012). Let \mathcal{F} be the collection of all probability distribution functions on \mathbb{R} , $F \in \mathcal{F}$ and $x \in \mathbb{R}$. In the univariate context, a depth measure is a function $D : \mathbb{R} \times \mathcal{F} \rightarrow [0, 1]$ such that, for any fixed F , $D(x, F)$ reaches their maximum value at the median of F , this is at x such that $F(x) = 1/2$, and decreases to the extent that x is farthest from the median. Examples of such univariate depth measures are

$$D(x, F) = 1 - \left| \frac{1}{2} - F(x) \right| \quad (1)$$

and

$$D(x, F) = 2(F(x)(1 - F(x))). \quad (2)$$

Denote by P to the generating law of the process X and by P_t to the marginal distribution of $X(t)$, this is $P_t(x) = \mathbb{P}(X(t) \leq x)$. Given a univariate depth measure D , the Integrated Functional Depth of X with respect to P is defined as

$$\text{IFD}(X, P) = \int_0^1 D(X(t), P_t) w(t) dt, \quad (3)$$

w being a weight function that integrates to one (Claeskens et al., 2014). It is worth mentioning that when $w \equiv 1$, and D is defined by Equation (1), the integrated functional depth corresponds to

the seminal Fraiman and Muñiz functional depth (Fraiman and Muniz, 2001). When D is defined by Equation (2), the corresponding IFD is the famous Modified Band Depth with bands formed by two curves (López-Pintado et al., 2010).

Define $\mathcal{J}(t) = \{1 \leq j \leq n : t \in O_j\}$. Suppose $\mathcal{J}(t) \neq \emptyset$ and let $q(t)$ be the cardinality of $\mathcal{J}(t)$. Denote by $F_{\mathcal{J}(t)}$ to the empirical distribution function of the univariate sample $\{X_j(t) : j \in \mathcal{J}(t)\}$. This is the probability distribution that assigns constant mass equals to $1/q(t)$ to each available observation at time t . Then, for any pair (X_i, O_i) and a given univariate depth D , we consider the empirical Partially Observed Integrated Functional Depth restricted to O_i (Elías et al., 2021b) defined by

$$\text{POIFD}(X_i, O_i) = \frac{\int_{O_i} D(X(t), F_{\mathcal{J}(t)}) q(t) dt}{\int_{O_i} q(t) dt}. \quad (4)$$

In line with the approach for dynamic updating introduced by Elías et al. (2021c), we search for a set \mathcal{J} of sample curves, as big as possible, such that $i \notin \mathcal{J}$ and:

1) (X_i, O_i) is deep in $\{(X_j, O_j) : j \in \mathcal{J} \cup \{i\}\}$, the deepest if possible. For measuring depth here we use the Partially Observed Integrated Functional Depth restricted to O_i defined in (4).

2) (X_i, O_i) is enveloped by $\{(X_j, O_j) : j \in \mathcal{J}\}$ as much as possible. Here, we say (X_i, O_i) is *more enveloped* by $\{(X_j, O_j) : j \in \mathcal{J}\}$ than by $\{(X_j, O_j) : j \in \mathcal{J}'\}$ if and only if

$$\lambda \left(\left\{ t \in O_i : \min_{j \in \mathcal{J}} X_j(t) \leq X_i(t) \leq \max_{j \in \mathcal{J}} X_j(t) \right\} \right) > \lambda \left(\left\{ t \in O_i : \min_{j \in \mathcal{J}'} X_j(t) \leq X_i(t) \leq \max_{j \in \mathcal{J}'} X_j(t) \right\} \right),$$

with λ being the Lebesgue measure on \mathbb{R} .

3) $\{(X_j, O_j) : j \in \mathcal{J}\}$ contains near curves to (X_i, O_i) , as many as possible. For measuring nearness, we use *mean L_2 distance* between POFD. This is,

$$\|(X_i, O_i) - (X_j, O_j)\| = \frac{\sqrt{\int_{O_i \cap O_j} |X_i(t) - X_j(t)|^2 dt}}{\lambda(O_i \cap O_j)}. \quad (5)$$

Algorithm 1 provides a set of curves with the three features above that we call the *i-curve envelope* and denote by \mathcal{J}_i from now on. The algorithm is a variation of Algorithm 1 of Elías et al. (2021c), adapted to POFD. Algorithm 1 iteratively selects as many sample curves as possible, from the nearest to the farthest to (X_i, O_i) , for enveloping (X_i, O_i) and increasing its depth.

Figure 1 illustrates how Algorithm 1 works. For there, we consider the first, second and final iteration of two runs from the algorithm based on 1000 i.i.d. trajectories of a Gaussian process. We considered partially observed curves for the run shown in the left panels by removing six random intervals of the observation domain. For the run shown in the right panels, we considered missing data uniformly on the observation domain. On average, only 50% of each curve were observed for both runs. The partially observed function we intend to reconstruct is colored in red and plotted

Algorithm 1 Input: $i, \{(X_j, O_j) : 1 \leq j \leq n\}$. Output: \mathcal{J}

Initialize $f = (X_i, O_i), \mathcal{Y} = \{(X_j, O_i \cap O_j) : j \neq i\}, \mathcal{J} = \emptyset$ and $D(f|\mathcal{J}, i) = 0$
while size of $\mathcal{Y} \geq 2$ **do**
 Let y' be the nearest curve to f from \mathcal{Y} and $\mathcal{N} = \{y'\}$
 for $y \in \mathcal{Y} \setminus \{y'\}$, from the nearest curve to the farthest from f , **do**
 $j_y = \{j : (X_j, O_i \cap O_j) = y\}$
 $\mathcal{J}^+ = \mathcal{J} \cup \{j : (X_j, O_i \cap O_j) \in \mathcal{N}\}$
 if f is more enveloped by $\mathcal{N} \cup \{y\}$ than by \mathcal{N} or $O_{j_y} \setminus \left(\cup_{j \in \mathcal{J}^+} O_j\right) \neq \emptyset$ **then**
 $\mathcal{N} = \mathcal{N} \cup \{y\}$
 end if
 end for
 if $D(f|\mathcal{J} \cup \mathcal{N}, i) \geq D(f|\mathcal{J}, i)$ **then**
 $\mathcal{J} = \mathcal{J} \cup \{j : (X_j, O_i \cap O_j) \in \mathcal{N}\}$
 end if
 $\mathcal{Y} = \mathcal{Y} \setminus \mathcal{N}$
end while

entirely in the bottom panels jointly with its estimation that we describe how to compute below.

2.3 Reconstruction of missing parts

For estimating the unobserved part of X_i , this is (X_i, M_i) , we use the same approach used for dynamic updating (Elías et al., 2021c). The estimator is a weighted functional mean from data of the curve envelope. Only here, these functional data may be partially observed. Specifically, these data are $\{(X_j, M_i \cap O_j) : j \in \mathcal{J}_i\}$. Consider $\mathcal{J}_i(t) = \{j \in \mathcal{J}_i : t \in O_j\}$, assume $\mathcal{J}_i(t) \neq \emptyset$ for all $t \in O_i$, and let $\delta = \min_{j \in \mathcal{J}_i} \|(X_i, O_i) - (X_j, O_j)\|$. Then, we estimate X_i on M_i by

$$\hat{X}_i^\theta(t) = \frac{\sum_{j \in \mathcal{J}_i(t)} w_j X_j(t)}{\sum_{j \in \mathcal{J}_i(t)} w_j}, \quad \text{with } w_j = \exp\left(\frac{-\theta \|(X_i, O_i) - (X_j, O_j)\|}{\delta}\right). \quad (6)$$

This estimator is a version of the envelope projection with exponential weights (see Elías et al., 2021c, Equation (2)), adapted to the partially observed data context. The parameter θ is chosen by minimizing the mean squared prediction error (MSE). In practice, if \hat{O}_i is the observational set where \hat{X}_i can be computable, this is $\cup_{j \in \mathcal{J}_i} (O_i \cap O_j)$, then

$$\theta = \arg \min_{\nu} \sum_{i=1}^n \|(X_i, O_i) - (\hat{X}_i^\nu, \hat{O}_i)\|^2.$$

As an illustration, the bottom panels of Figure 1 show reconstructions of missing parts of the two simulated cases discussed above.

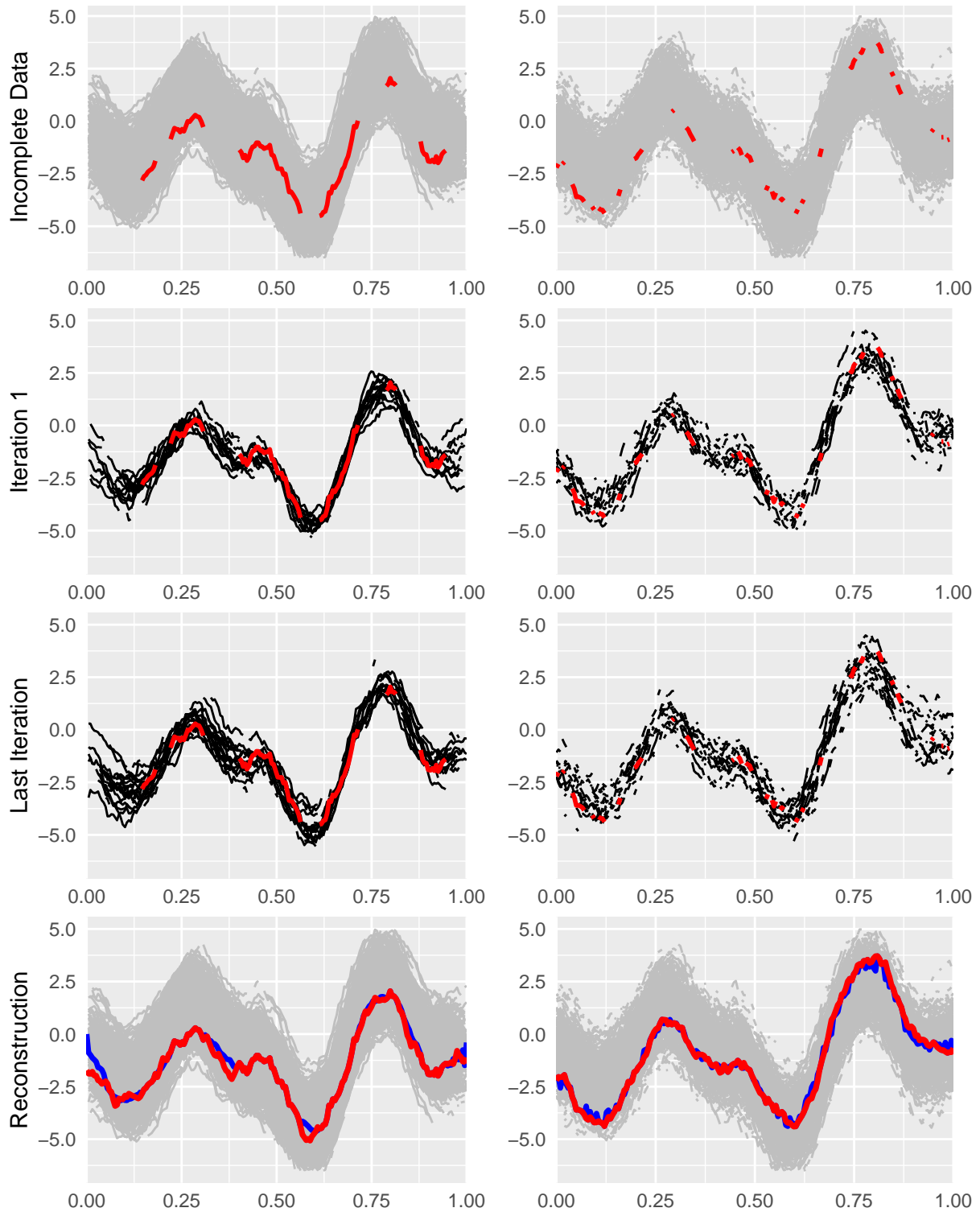


Figure 1: In the top panels, an illustration of how Algorithm 1 works. The sample curves correspond to 1000 i.i.d. trajectories of a Gaussian process. We considered partially observed curves for the left panels by removing six random intervals from $[0, 1]$. For the right panels, we considered missing data uniformly. On average, only 50% of each curve was observed for both runs. The partially observed function that we reconstructed is colored in red and plotted entirely in the bottom panels jointly with its estimation. (in blue)

3 Results

We compare results obtained by using the depth-based method with those obtained from studies by Kraus (2015) and Kneip and Liebl (2020). Kraus (2015) propose a regularized regression model to predict the principal component scores (Reg. Regression) whereas Kneip and Liebl (2020) introduce a new class of reconstruction operators that are optimal (Opt. Operator). The two methods were implemented by using the R-codes available at https://is.muni.cz/www/david.kraus/web_files/papers/partial_fda_code.zip and <https://github.com/lidom/ReconstPoFD>. The depth for partially observed curves and the data generation settings are implemented using the R-package `fdaPOIFD` of Elías et al. (2021a).

Subsection 3.1 introduces the simulation setting, the data generation process for POFD and shows results with synthetic data. Subsection 3.2 uses the same simulation settings but applied to AEMET temperatures data. Additionally, it illustrates the reconstruction of some yearly temperature curves that are partially observed in reality. Finally, Subsection 3.3 presents another real case study where Japanese age-specific mortality functions are reconstructed.

3.1 Simulation study

Let us denote by $c\%$ the percentage of sample curves that are partially observed. We remark that benchmark methods perform better as the parameter c is larger. This is because these reconstruction methods strongly depend on the information of the completely observed curves to estimate the covariance or the components of its eigendecomposition. However, the depth-based method can handle the case $c = 0$, i.e., there are no complete functions in the sample. Therefore, results for this case are reported without comparison.

For our simulation study, we considered two Missing-Completely-at-Random procedures for generating partially observed data. These procedures have previously been used in the literature (Elías et al., 2021b) and are in line with the partial observability of the real case studies. They are:

Random Intervals, with which $c\%$ of the sample curves is observed on a number m of random disjointed intervals of $[0, 1]$.

Random points, with which $c\%$ of the functions is observed on a very sparse random grid. First, we apply these observability patterns to simulated trajectories. Concretely, we consider a Gaussian process $X(t) = \mu(t) + \epsilon(t)$ where $\epsilon(t)$ is a centered Gaussian process with covariance kernel $\rho_\epsilon(s, t) = \alpha e^{-\beta|s-t|}$ for $s, t \in [0, 1]$. The functional mean $\mu(t)$ is a periodic function randomly generated by a centered Gaussian process with covariance $\rho_\mu(s, t) = \sigma e^{-(2 \sin(\pi|s-t|)^2 / l^2)}$. Thus, each sample will present different functional means. The set of parameters used for our study were $\beta = 2$, $\alpha = 1$, $\sigma = 3$ and $l = 0.5$. Example of the generated trajectories by this model are those shown in Figure 1.

We considered small and large sample sizes for the study by making $n = 200$ and $n = 1000$. Also, we considered different percentages of observed curves that were partially observed. Specifically, we tested with $c = 0, 25, 50$ and 75 . In addition, we considered different percentages of time on which the incomplete curves of a sample were observed. Henceforth, we term this percentage by $p\%$. We considered $p = 25, 50$ and 75 for small samples but only $p = 25$ and 50 for large samples. This is due to the computational cost of the benchmark methods when $n = 1000$ and $p = 75$. Note that this parameter setting implies the highest computational cost for estimating covariance functions. Finally, we replicate 100 samples of each data set for estimating median values of MSE.

Table 1 presents results for $n = 200$. It shows MSE from the Gaussian data and points out the superiority of the Reg. Regression method (Kraus, 2015) when covariance function is simple to estimate, as is the case of the exponential decay covariance function involved in these data (see left panel of Figure 2). We remark that, even in this case, depth-based is lightly better than the Opt. Operator method (Kneip and Liebl, 2020). When all the functions of the sample are partially observed ($c = 0\%$), only the depth-based method can provide a reconstruction and, surprisingly, the MSE remains reasonably similar to those cases with a proportion of complete functions significantly large ($c = 25, 50, 75\%$). Similar results are obtained with larger sample sizes.

Table 1: Median values of mean square errors over 100 pseudo-random replicates. Each replicate is composed of 200 curves. A dash (-) represents that the method cannot produce any reconstruction. The partially observed samples are obtained by observing $p\%$ of the total discrete realization points (Random Points). The smallest error is bolded for each combination of c and p .

Method	$c = 75$			$c = 50$			$c = 25$			$c = 0$		
	$p = 25$	50	75	25	50	75	25	50	75	25	50	75
Depth-based	0.153	0.138	0.133	0.169	0.144	0.137	0.197	0.154	0.14	0.259	0.168	0.143
Opt. Operator	0.159	0.16	0.247	0.179	0.191	0.246	0.187	0.185	0.256	-	-	-
Reg. Regression	0.059	0.054	0.049	0.075	0.07	0.06	0.124	0.111	0.086	-	-	-

3.2 Case study: Reconstructing AEMET temperatures

Spanish Agency of Meteorology (AEMET) provides meteorological variables recorded from different stations in the whole Spanish territory (see <http://www.aemet.es/es/portada>). This analysis focus on maximum daily temperatures of 73 stations located in the capital of provinces. Following the literature of FDA, we consider this data as a functional data set where each function are the temperatures of each complete year (Febrero-Bande and Oviedo de la Fuente, 2012; García-Portugués et al., 2014). Some of the curves are partially observed in the historical data, and our goal is to reconstruct the data set.

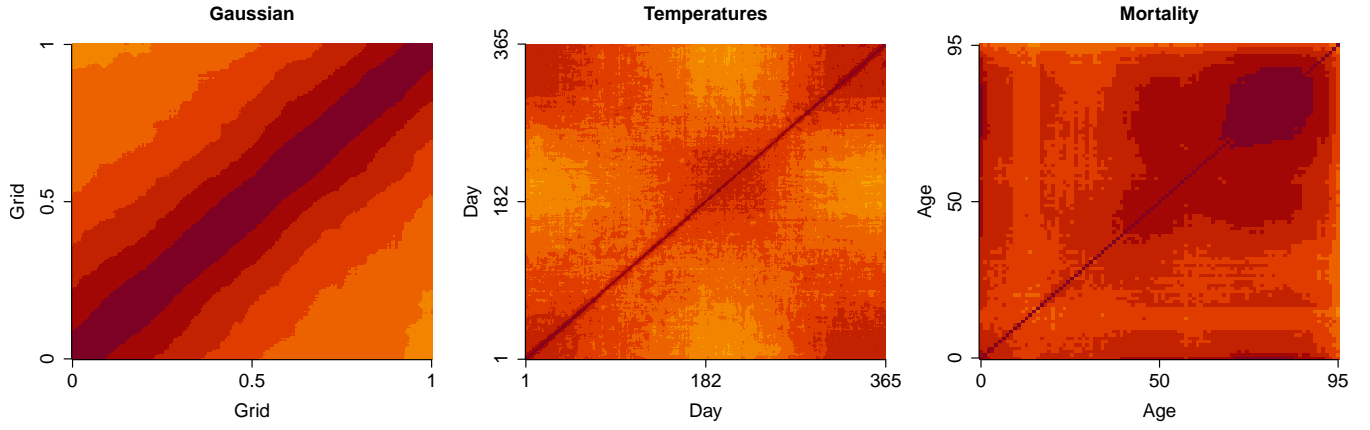


Figure 2: Covariance estimations based on the available functions are completely observed. Left panel, Gaussian processes with an exponential decay covariance. Central panel: Spanish daily temperatures with lower covariance values in Spring and Autumn periods and higher covariance in Summer and Winter. Right panel: Japanese age-specific mortality rates with higher correlations at the oldest ages.

Temporal data availability depends from one station to the other. For example, Madrid-Retiro station is the oldest station, being monitored from 1893. However, Ceuta from 2003. In total, we consider a set of 2786 entirely observed curves of different years and weather stations. This large sample of complete functions allows reproducing the simulation in Subsection 3.1 by randomly generating random functional samples. To do that, we randomly generate 100 samples of curves without replacement. The results for sample sizes of $n = 200$ and $n = 1000$ are in Table 2. Unlike Gaussian data, the depth-based method seems to be superior to the competitors in the simulation with AEMET data. Only for high proportions of complete functions $c = 75$ and small sample size $n = 200$, Kraus's (2015) method was superior, becoming the depth-based method superior for smaller values of c or larger sample sizes $n = 1000$. These results can be explained by the complex structure of AEMET data as shown in the center panel of Figure 2.

Table 2: Median values of mean square errors over 100 replications. Each replicate is composed of 1000 and 200 curves (results between parenthesis). A dash (-) represents that the method cannot produce any reconstruction. The partially observed samples are obtained by observing $p\%$ of the total discrete realization points (Random Points).

Method	$c = 75$		$c = 50$		$c = 25$		$c = 0$	
	$p = 25$	50	25	50	25	50	25	50
Depth-based	5.393 (9.639)	4.920 (9.099)	6.384 (10.879)	5.274 (9.585)	7.874 (12.555)	6.321 (10.079)	10.252 (14.691)	7.606 (10.900)
Opt. Operator	13.081 (13.184)	13.403 (13.530)	13.201 (13.296)	13.442 (13.493)	13.259 (13.412)	13.229 (13.436)	-	-
Reg. Regression	6.834 (9.508)	5.41 (8.826)	7.349 (10.842)	5.944 (10.472)	8.617 (13.577)	8.217 (13.251)	-	-

Table 3 shows the same simulation setup with AEMET data but under the Random Interval setting and small sample size. In this setting, we generate partially observed data for a different number of observed intervals (m), percentages of completely observed curves (p), and mean

observability percentage of each partially observed curve (c). The result shows that when $p = 25$ the Reg. The regression method typically performs better than the competitors. This is because our implementation of the partially observed setting produces a sample of curves not as densely distributed in the extremes of the domain as it is in the middle of the domain. Then, for small p to extrapolate using the depth-based method to dense part of the domain worsens the results. However, when p increases, our implementation produces a sample of partially observed curves covering the complete domain densely, and the depth-based method outperforms.

Table 3: Median values of the mean squared error after 100 replications. This table summarizes the exercise considering random samples from the fully observed AEMET data set. Each replicate is composed of 200 functional observations. The partially observed samples are obtained by restricting each function to m intervals of total length $p\%$ of the domain (Random Intervals).

Intervals	Method	$c = 75$			$c = 50$			$c = 25$		
		$p = 25$	50	75	25	50	75	25	50	75
$m = 1$	Depth-based	13.359	10.037	8.999	15.597	11.224	9.690	18.122	12.903	10.884
	Opt. Operator	16.041	12.862	10.998	16.105	13.119	10.979	16.567	13.366	11.168
	Reg. Regression	14.420	11.033	9.472	15.466	12.359	10.290	16.821	14.194	10.877
$m = 2$	Depth-based	13.546	10.363	8.975	16.935	11.076	9.621	19.415	12.347	10.385
	Opt. Operator	16.657	13.689	11.200	16.856	13.591	11.373	16.960	13.662	11.549
	Reg. Regression	13.369	11.394	9.542	14.439	12.393	10.597	16.074	14.228	12.422
$m = 4$	Depth-based	13.841	10.316	9.199	16.403	10.829	9.579	18.682	11.800	10.097
	Opt. Operator	16.164	13.665	12.126	16.088	13.689	11.953	16.105	13.563	11.962
	Reg. Regression	12.909	11.320	10.022	13.676	12.354	11.063	15.427	14.301	12.736

In Figure 3, we plot the reconstructions obtained by the three methods under consideration from one random sample. This was obtained by randomly taking 1000 curves from the total observed curves of the AEMET data. Then, we generated partially observed data by applying the Missing-Completely-at-Random procedure based on random intervals described above, with $m = 4$, $p = 50$, and $c = 50$. Finally, we randomly selected one function to reconstruct, namely, VALLADOLID/VILLANUBLA-1956, where VALLADOLID/VILLANUBLA refers to the location of the station and 1956 to the observation year. According to a general view of its shape, VALLADOLID/VILLANUBLA-1956 is completely plotted in red. In contrast, the reconstructions are only plotted on the four intervals where the curve was observed in our simulation. The top panels of the figure show output produced by the depth-based method (Depth-based in blue), Kneip and Liebl (2020) (Opt. Operator in green), by Kraus (2015) (Reg. Regression in black). The depth-based method is superior to the benchmark methods. The bottom panel of the figure shows some descriptive statistics related to the depth-based method. We show years used for reconstructing (the years of the curves into the envelope). The frequency of each year (number of curves into the envelope with the same year) is represented by a proportional blue bubble. Similarly, we show at the right side the locations of the curves into the envelope. From our understanding, all of them

have similar geographical features.

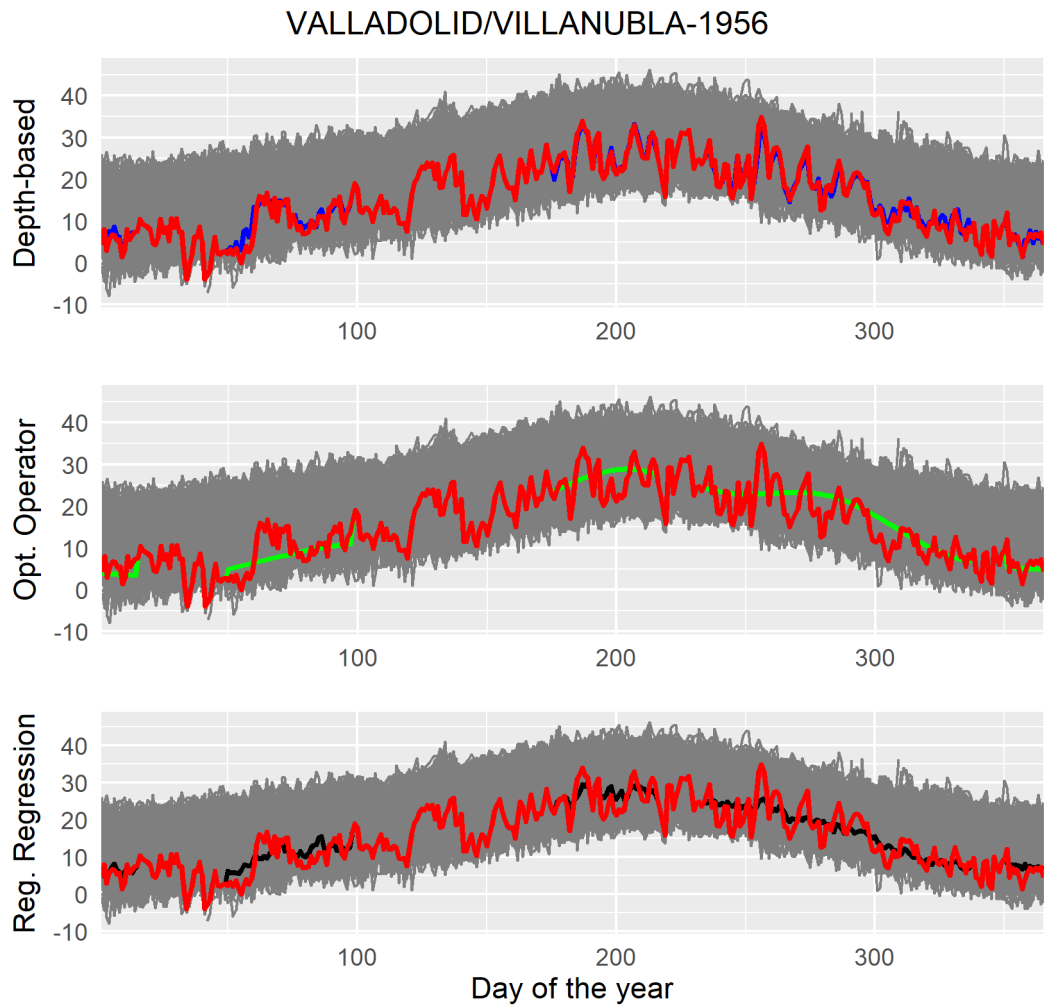


Figure 3: Simulated exercise reconstruction of “VALLADOLID/VILLANUBLA-1956”. Top panel presents the reconstruction by Kraus (2015) (black) and Kneip and Liebl (2020) (green). Middle panel, the reconstruction provided by the depth-based method. Bottom panel, the spatial (Spanish map) and temporal (bubble plot) descriptive analysis offered by the depth-based methodology and the envelope.

Finally, Figure 4 illustrates the actual case of “BURGOS/VILLAFRÍA-1943” a station that probably started operating in the middle of the year 1943. Consequently, only the year’s second half is recorded (red curve at the top panel). We apply the three reconstructing methods to complete the first half of the curve (Reg. Regression (Kraus, 2015) in black, Opt. Operator (Kneip and Liebl,

2020) in green, and the depth-based method in blue). The depth-based methodology supports the reconstruction with the additional information provided by the most important curves of the envelope. The subsample contains distant-past function from 1905 from MADRID-RETIRO station, more recent functions from the 90s from the same “BURGOS-VILLAFRÍA” station a bigger proportion of functions from 1943, belonging to the same year of the partially observed function to reconstruct.

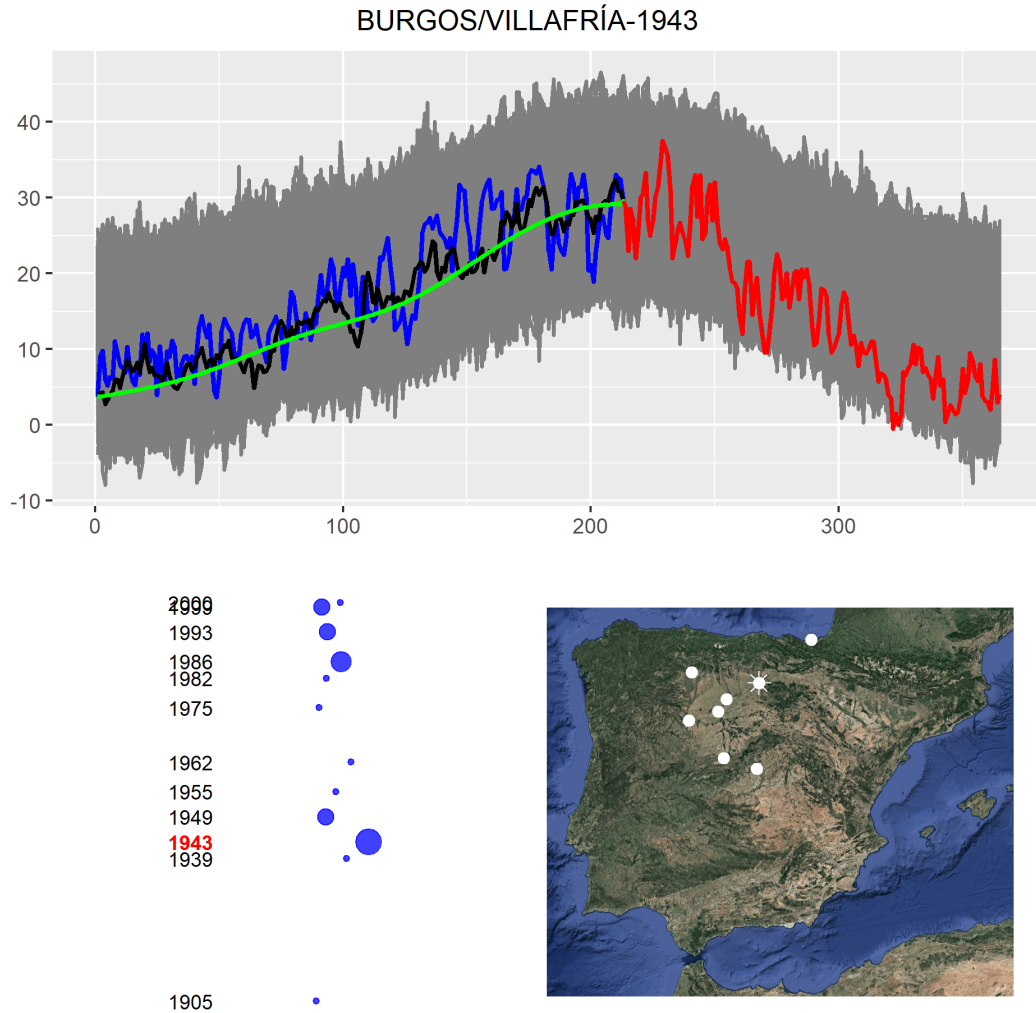


Figure 4: Real partially observed function, “BURGOS/VILLAFRÍA-1943”. Top panel: reconstructions by Kraus (2015) (in black) Kneip and Liebl (2020) (in green) and the depth-based method (in blue). The bottom panel shows the descriptive analysis of the most relevant curves in reconstructing “BURGOS/VILLAFRÍA-1943”. In the left part, time analysis (bubble plot of the involved years); in the right part, spatial analysis (map with the most relevant and involved stations).

3.3 Case study: Reconstructing Japanese mortality

The Human Mortality Data Set (<https://www.mortality.org>) provides detailed mortality and population data of 41, mainly in developed countries. Some countries also offer micro information by subdivision of the territory, providing challenging spatial and temporal information. In particular, the Japanese mortality data set (<http://www.ipss.go.jp/p-toukei/JMD/index-en.asp>) is

available for its 47 prefectures for males, females, and the total population.

A common FDA approach to analyze mortality data is to consider that each function is the yearly mortality for each age cohort (Shang and Hyndman, 2017; Shang and Haberman, 2018; Gao et al., 2019; Shang, 2019). With this configuration and arranging the 47 prefectures together, we deal with a male, female, or total Japanese mortality data set of size 2007. Of course, each prefecture does not have the same number of functions, and the range of observed years is also different. However, roughly, we have yearly mortality functions between 1975 and 2016.

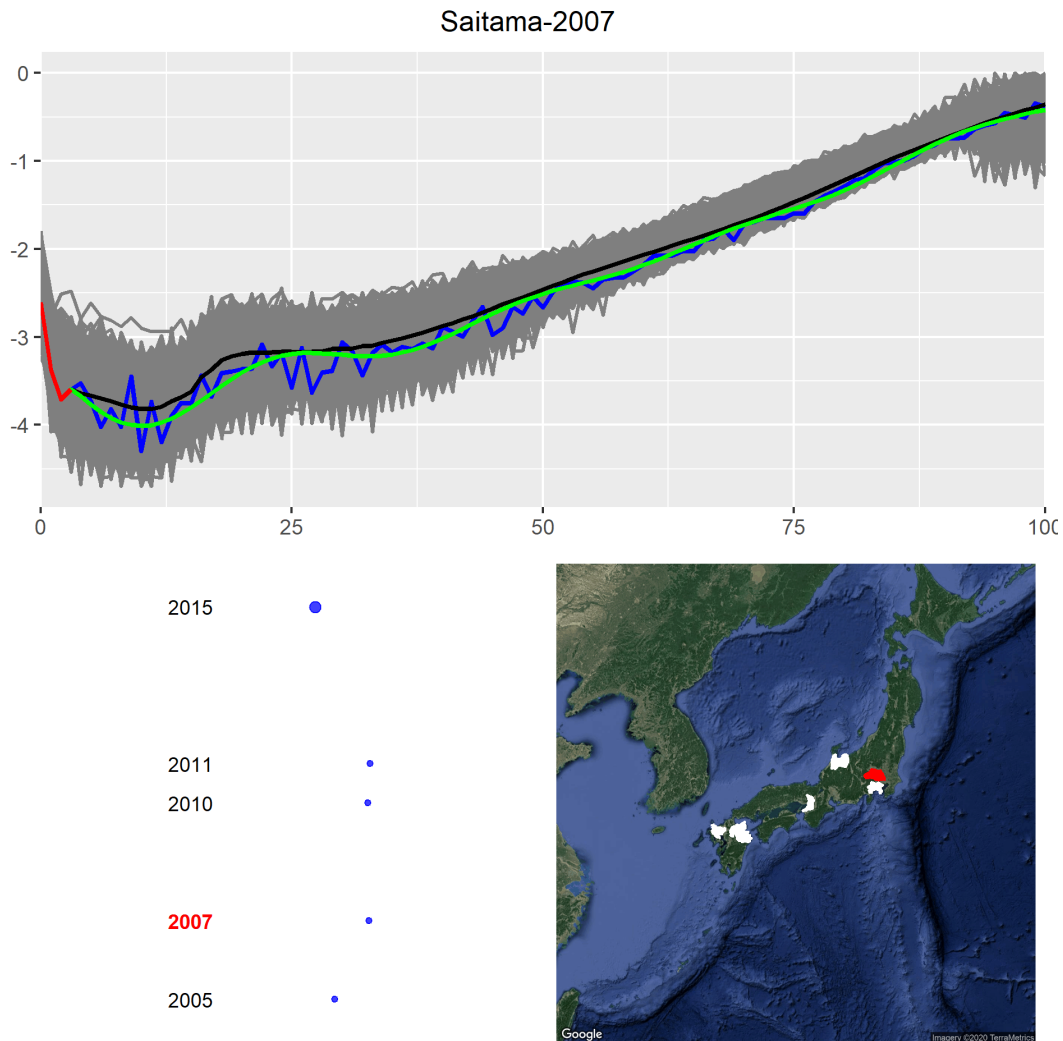


Figure 5: Reconstruction of the most poorly observed function of the sample, “Saitama-2007”. The top panel presents the reconstruction given by Reg. Regression method by Kraus (2015) (black), Opt. Operator method by Kneip and Liebl (2020) (green) and the depth-based method (blue). The bottom panel shows the year of the most important functions of the envelope, and the maps showing the corresponding prefectures, in red the one to be reconstructed.

In this case study, the poor availability of complete functions invalidates the possibility of doing a resampling exercise like the one we have done for the AEMET data set. Then, we are only able to illustrate some real situations. Figures 5 and 6 present two real reconstruction problems and the results obtained from the three methods. In Figure 5, we reconstruct the shortest available curve, “Saitama-2007”, that was only available in a very short interval of mortality rates for the youngest

cohorts. Reg. Regression (Kraus, 2015) and Opt. Operator (Kneip and Liebl, 2020) produce smooth results (black and green respectively). The depth-based method produces more spiky results in concordance with other available curves. The bottom panel presents the bubble plot illustrating the period of the envelope functions and the prefectures in the map. Figure 6 presents a case with the function “Tottori-2015” that is not observed in six intervals fragments (domain where only the red curve is visible).

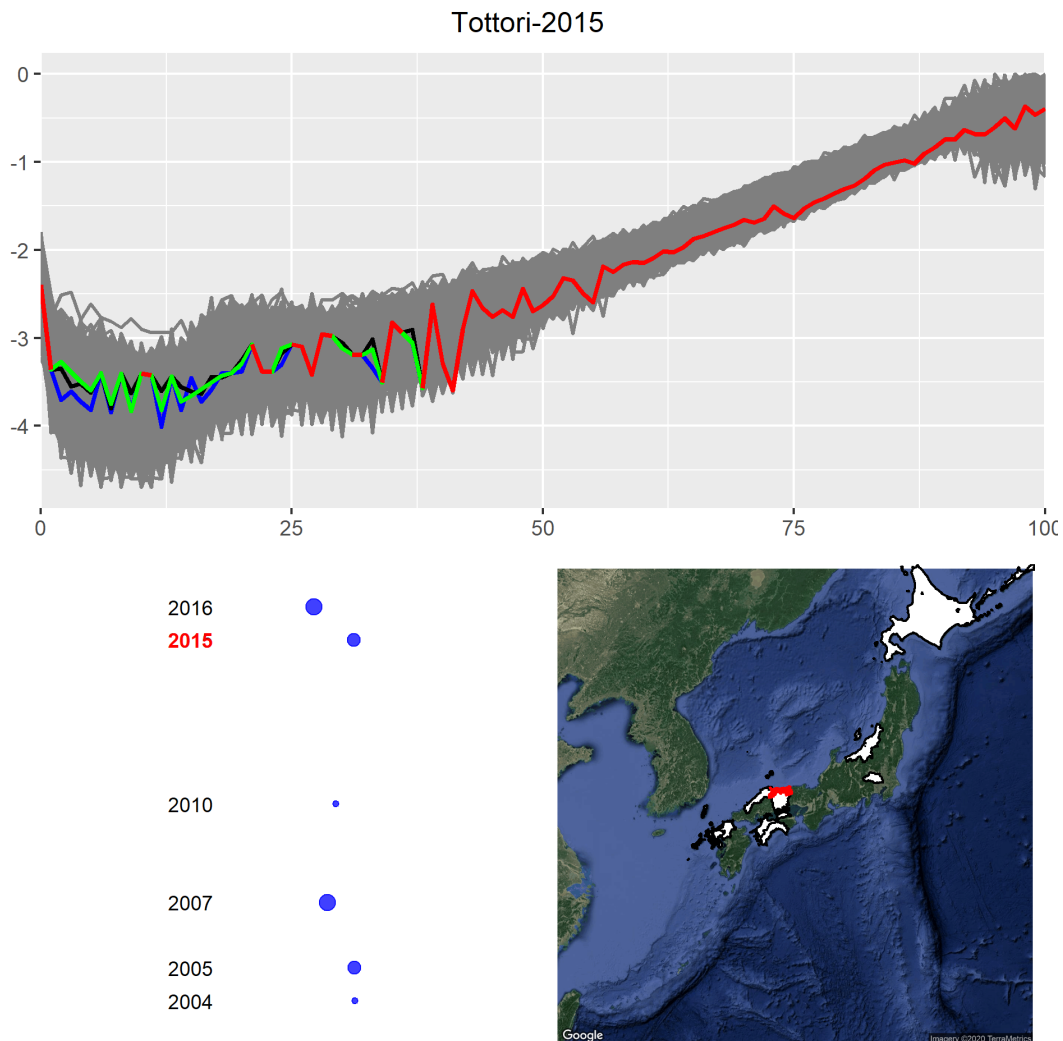


Figure 6: Real partially observed function of the sample observed in 6 fragments, Tottori-2015. The top panel presents the reconstruction given by Reg. Regression method by Kraus (2015) (black), Opt. Operator method by Kneip and Liebl (2020) (green) and the depth-based method (blue). The bottom panel shows the year of the most important functions of the envelope, and the right map shows its prefectures.

4 Conclusion

This article introduces a non-parametric method to reconstruct samples of incomplete functional data. Our proposal relies on the concept of depth for POFD to select a subset of sample curves that is defined to share shape and magnitude with the observed part of the curve to predict. We term this subset of sample curves as envelope, and we use them to proposed a point reconstruction

method based on a weighted average. These weights only depend on a parameter we set by minimizing the MSE where the curve to predict is observed.

We compare the performance of the new method with other alternatives of the literature. Our simulation exercises consider simulated and real data and various random procedures to generate incomplete data scenarios. The available reconstruction methods seem to be unbeatable in our settings when the covariance can be efficiently estimated. These favorable circumstances are exemplified with Gaussian processes with stationary covariance functions and other more complex covariance regimes, including a considerable proportion of completely observed curves. In contrast, our method outperforms when the covariance can not be properly estimated due to a richer covariance structure and highly scarce data settings. To show that, we test the methods under severe incomplete data settings and introduce more complex covariance structures. Particularly, we decrease the number of completely observed functions up to zero and consider real data with complex covariance structures such as yearly age-specific mortality and yearly temperature data. Finally, our simulation exercises show that our proposal can provide a reasonable reconstruction output when every function is partially observed or, in other words, when there are no complete functions in the sample.

The depth-based method requires the Missing-Completely-at-Random assumption, as it is standard in the literature. This assumption implies that the partially observed functions cover densely the reconstruction domain and that the observability process is not conditional to external information. Future research could allow for specific relationships between the functional process and the process that generates partial observability. In addition, the depth-based algorithm requires a notion of proximity between POFD that we fill with a L_2 distance between the observed segments. Developments along this line would also be valuable for our proposal.

In summary, this article provides an alternative data-driven and model-free method to reconstruct partially observed functional data preferable under challenging scenarios like the ones presented here. Last but not least, we believe that the interpretability of the results might be helpful to provide different insides into the data under analysis.

Acknowledgments

Antonio Elías was supported by the Ministerio de Educación, Cultura y Deporte under grant FPU15/00625 and the research stay grant EST17/00841. Antonio Elías and Raúl Jiménez were partially supported by the Spanish Ministerio de Economía y Competitividad under grant ECO2015-66593-P. Part of this article was conducted during a stay at Australian National University. Antonio Elías is grateful to Han Lin Shang for his hospitality and insightful and constructive discussions.

References

- Claeskens, G., Hubert, M., Slaets, L., and Vakili, K. (2014). Multivariate functional halfspace depth. *Journal of the American Statistical Association: Theory and Methods*, 109(505):411–423.
- D’Amato, V., Piscopo, G., and Russolillo, M. (2011). The mortality of the Italian population: Smoothing techniques on the Lee-Carter model. *Annals of Applied Statistics*, 5(2A):705–724.
- Delaigle, A. and Hall, P. (2013). Classification using censored functional data. *Journal of the American Statistical Association: Theory and Methods*, 108(504):1269–1283.
- Delaigle, A. and Hall, P. (2016). Approximating fragmented functional data by segments of markov chains. *Biometrika*, 103(4):779–799.
- Elías, A., Jiménez, R., Paganoni, A., and Sangalli, L. (2021a). *fdaPOIFD: Partially Observed Integrated Functional Depth*. R package version 1.0.0. URL: <https://CRAN.R-project.org/package=fdaPOIFD>.
- Elías, A., Jiménez, R., Paganoni, A. M., and Sangalli, L. M. (2021b). Integrated depth for partially observed functional data. *Submitted to Journal*.
- Elías, A., Jiménez, R., and Shang, H. L. (2021c). On projection methods for functional data forecasting. *Journal of Multivariate Analysis*, in press.
- Febrero-Bande, M. and Oviedo de la Fuente, M. (2012). Statistical computing in functional data analysis: The R package *fda.usc*. *Journal of Statistical Software*, 51(4):1–28.
- Ferraty, F. and Vieu, P. (2006). *Nonparametric Functional Data Analysis: Theory and Practice*. Springer-Verlag New York.
- Fraiman, R. and Muniz, G. (2001). Trimmed means for functional data. *TEST*, 10(2):419–440.
- Gao, Y., Shang, H. L., and Yang, Y. (2019). High-dimensional functional time series forecasting: An application to age-specific mortality rates. *Journal of Multivariate Analysis*, 170:232–243.
- García-Portugués, E., González-Manteiga, W., and Febrero-Bande, M. (2014). A goodness-of-fit test for the functional linear model with scalar response. *Journal of Computational and Graphical Statistics*, 23(3):761–778.
- Goldberg, Y., Ritov, Y., and Mandelbaum, A. (2014). Predicting the continuation of a function with applications to call center data. *Journal of Statistical Planning and Inference*, 147:53–65.
- Hubert, M., Rousseeuw, P. J., and Vanden Branden, K. (2005). Robpca: A new approach to robust principal component analysis. *Technometrics*, 47(1):64–79.

- Human Mortality Database (2021). *University of California, Berkeley (USA) and Max Planck Institute for Demographic Research (Germany)*. Available at www.mortality.org. Accessed at July 21, 2021.
- James, G., Hastie, T., and Sugar, C. (2000). Principal component models for sparse functional data. *Biometrika*, 87(3):587–602.
- James, G. M. and Hastie, T. J. (2001). Functional linear discriminant analysis for irregularly sampled curves. *Journal of the Royal Statistical Society: Series B (Statistical Methodology)*, 63(3):533–550.
- Kneip, A. and Liebl, D. (2020). On the optimal reconstruction of partially observed functional data. *The Annals of Statistics*, 48(3):1692–1717.
- Kraus, D. (2015). Components and completion of partially observed functional data. *Journal of the Royal Statistical Society: Series B (Statistical Methodology)*, 77(4):777–801.
- Li, J., Cuesta-Albertos, J. A., and Liu, R. Y. (2012). DD-classifier: Nonparametric classification procedure based on DD-plot. *Journal of the American Statistical Association: Theory and Methods*, 107(498):737–753.
- Liebl, D. and Rameseder, S. (2019). Partially observed functional data: The case of systematically missing parts. *Computational Statistics & Data Analysis*, 131:104–115. High-dimensional and functional data analysis.
- Liu, R. Y. (1990). On a notion of data depth based on random simplices. *The Annals of Statistics*, 18(1):405–414.
- Liu, R. Y., Parelius, J. M., and Singh, K. (1999). Multivariate analysis by data depth: Descriptive statistics, graphics and inference. *The Annals of Statistics*, 27(3):783–840.
- López-Pintado, S., Romo, J., and Torrente, A. (2010). Robust depth-based tools for the analysis of gene expression data. *Biostatistics*, 11(2):254–264.
- Ramsay, J. and Silverman, B. (2005). *Functional Data Analysis*. Springer, New York, 2nd edition.
- Rousseeuw, P. J., Ruts, I., and Tukey, J. W. (1999). The bagplot: A bivariate boxplot. *The American Statistician*, 53(4):382–387.
- Sangalli, L. M., Secchi, P., and Vantini, S. (2014). AneuRisk65: A dataset of three-dimensional cerebral vascular geometries. *Electronic Journal of Statistics*, 8(2):1879–1890.
- Sangalli, L. M., Secchi, P., Vantini, S., and Veneziani, A. (2009). A case study in exploratory functional data analysis: Geometrical features of the internal carotid artery. *Journal of the American Statistical Association: Applications and Case Studies*, 104(485):37–48.

- Serfling, R. J. (2006). Multivariate symmetry and asymmetry. In Kotz, S., Read, C. B., Balakrishnan, N., Vidakovic, B., and Johnson, N. L., editors, *Encyclopedia of Statistical Sciences*, volume 8, pages 5338–5345. Wiley-Interscience, Hoboken, New Jersey, 2nd edition.
- Shang, H. L. (2019). Visualizing rate of change: An application to age-specific fertility rates. *Journal of the Royal Statistical Society: Series A (Statistics in Society)*, 182(1):249–262.
- Shang, H. L. and Haberman, S. (2018). Model confidence sets and forecast combination: An application to age-specific mortality. *Genus*, 74(1):19.
- Shang, H. L. and Hyndman, R. J. (2017). Grouped functional time series forecasting: An application to age-specific mortality rates. *Journal of Computational and Graphical Statistics*, 26(2):330–343.
- Yao, F., Muller, H. G., and Wang, J. L. (2005). Functional data analysis for sparse longitudinal data. *Journal of the American Statistical Association: Theory and Methods*, 100(470):577–590.
- Zuo, Y. and Serfling, R. (2000). General notions of statistical depth function. *The Annals of Statistics*, 28(2):461–482.